Hindawi
Discrete Dynamics in Nature and Society
Volume 2023, Article ID 3457612, 14 pages
https://doi.org/10.1155/2023/3457612

Research Article

Hopf Bifurcation Analysis of a Continuous Investment Update Project Model

Debao Gao

College of Science, Heilongjiang Bayi Agricultural University, Daqing 163319, China

Correspondence should be addressed to Debao Gao; godebao@126.com

Received 5 May 2023; Revised 30 July 2023; Accepted 23 August 2023; Published 31 August 2023

Academic Editor: Emilio Jiménez Macías

Some investment projects aim not only to produce goods but more importantly, to update and efficiently supply products in accordance with market demand. A double time delay differential dynamics model is formulated for continuous renewal investment projects based on the flowchart of the capital appreciation process and the assumed transfer functions. By analyzing the mathematical model, it can be determined that a unique local asymptotically stable positive equilibrium point exists for the continuous investment project. In accordance with the Hopf branching theorem, the model displays periodic behavior in proximity to its positive equilibrium point under certain conditions. The simulation results are compared under various conditions, and the validity of the relevant conclusions is confirmed.

1. Introduction

The act of investment is widely recognized as one of the most prevalent and pivotal economic endeavors in contemporary society. The hysteresis effect of investment income is a crucial factor contributing to economic fluctuations. The objective of investors is to maximize their return on investment. To maximize the long-term profitability of the project, it is imperative to enhance the competitiveness of its products through regular updates in order to thrive in the market.

Using the investment in the antivirus software project as an example, due to the continuous emergence of viruses, it is imperative to consistently update the antivirus functionality of such software. Otherwise, it risks being rendered obsolete by market forces. There are numerous comparable projects that cannot all be enumerated. The process of updating project products involves two crucial components: research and development (R&D) and production, both of which necessitate financial support. Sustained investment is imperative for the continuous enhancement of products. The realization of investment returns is contingent upon the effective supply of project products to meet demand. Failure to effectively supply products to meet demand may result in investment failure.

The objective of this study is to utilize mathematical models to investigate the phenomenon of investment characterized by delayed returns and continuous infusions of capital.

Numerous mathematical models have been developed to address the investment problem. Classical models, such as the geometric Brownian motion model [1–3] and the constant elasticity of variance model [4], are commonly employed in financial modeling. Vigna and Haberman [1] utilized the geometric Brownian motion model and stochastic optimal control principle to investigate the optimal investment of pension asset allocation plans in discrete time. Building on this foundation, Haberman and Vigna [2] assumed a hypothetical asset allocation model that invests in two types of assets—risky assets and risk-free assets— and derived an asset allocation formula for the optimal investment problem. Thomson [3], assuming continuous rather than discrete time, applied dynamic programming principles to obtain the optimal investment strategy with the goal of maximizing expected utility at retirement. The CEV (constant elasticity of variance) model represents an enhanced version of the GBM model for pricing risk assets. Cox et al. [4] proposed that the CEV model has been utilized in the computation of various theories, including option pricing and implied volatility. In addition to the CEV model,

another investment model that has garnered significant attention is the Heston stochastic volatility model, initially proposed by Heston [5]. The key distinction between the Heston model and the CEV model lies in their consideration of random volatility for risk assets as well as assuming randomness in return rates. To better align with real-world financial market dynamics, volatility is assumed to follow a mean-reverting process, enabling a more accurate explanation of phenomena such as peaks and fat tails observed in financial markets. Furthermore, this model allows for the calibration of its parameters through options traded within the market. Lin and Yang [6] and Zhang et al. [7], among others, incorporated the Heston model into their investigation of DC pension schemes, exploring its optimal investment problem and proposing an optimal investment-consumption strategy.

The classical model presented above is subject to certain limitations. In the Heston model, risk asset prices and volatilities are stochastic, with a complex conditional distribution that poses significant challenges for solution. The CEV model in its current form fails to adequately incorporate multiple factors and lacks the ability to promptly capture real-time market dynamics, thus limiting its applicability in reflecting the most recent changes in financial markets. The lag in investment returns is inadequately captured.

In recent years, the differential dynamics theory has been applied by scholars (see [8–11]) to investigate various economic issues. For example, the authors in [8–10] used the time lag theory [12] to establish a business cycle model and explore the laws of the business economy. The stability analysis of the competition model with two delays is presented in [11]. The inclusion of a time delay in the differential dynamics model not only alters the stability of the original model but also induces oscillatory or periodic cyclic solutions, making it more suitable for practical implementation in commercial systems based on delay differential equations.

The pursuit of investment income serves as the impetus driving investors to actively engage in projects, while the key to realizing investment benefits lies in the effective supply of project products to meet demand. According to the flow of investment funds, these funds are allocated towards research and development projects as well as commodity production endeavors. Successful research and development projects are utilized in the production of commodities, which are subsequently supplied to meet market demand. The value of capital generally exhibits a gradual increase throughout its flow. In the event of an unsuccessful investment, the value of the currency will gradually depreciate throughout its circulation. Similar to the spread of infectious diseases [13–17], the number of infected individuals may increase, decrease, or stabilize over time. Therefore, this paper employs the theory of infectious disease dynamics to investigate the dynamic model of continuous project investment renewal.

The present study primarily contributes to the research in two key aspects.

(1) The differential dynamics theory is employed to investigate the dynamic changes of capital during the investment process.

(2) The temporal intervals required for research or production are expressed with varying degrees of latency.

It is worth noting that the conceptual framework adopted in this paper diverges from that in [18]. While the study [18] primarily examines the flow direction of funds, our study places greater emphasis on analyzing shifts in supply and demand dynamics. This approach aligns more closely with the rational consumer's perspective.

2. Model Construction and Its Basic Results

This article solely focuses on long-term operational projects that necessitate consistent investment. The investment project is presumed to encompass four primary components: funding, research and development (R&D), production, and demand. To establish the mathematical model, it is necessary to make the following assumptions for the four components:

(1) Assuming $F(t), R(t), P(t)$, and $D(t)$ represent the amount of funding, R&D, production, and demand at time t, respectively.

(2) The average research and development (R&D) duration of the project is τ_1, while the average production time for the product is τ_2.

(3) The fund amount is subject to an upper limit, determined by the input rate of $F \cdot (u - vF)$, and the transfer rate to R&D is denoted as kF.

(4) The rate of R&D consumption is denoted as aR, while the transfer rate to production is represented by mR.

(5) The consumption rate of the production part is denoted as bP, while the effective supply rate from the production part to the demand part is represented by nPD.

(6) The consumption rate of the demand component for the product is denoted as cD.

Based on assumptions (1)–(6), a warehouse diagram can be constructed to illustrate the relationships among fund, R&D, production, and demand, as depicted in Figure 1.

The differential dynamic model presented in Figure 1 can be derived as follows:

$$\begin{cases} \dfrac{\mathrm{d}F}{\mathrm{d}t} = F(t)(u - \mathrm{vF}(t)) - \mathrm{kF}(t), \\ \dfrac{\mathrm{d}R}{\mathrm{d}t} = \mathrm{kF}(t) - aR(t) - mR(t-\tau_1), \\ \dfrac{\mathrm{d}P}{\mathrm{d}t} = mR(t-\tau_1) - bP(t) - nP(t-\tau_2)D(t), \\ \dfrac{\mathrm{d}D}{\mathrm{d}t} = nP(t-\tau_2)D(t) - cD(t), \end{cases} \tag{1}$$

where $u, v, k, m, n, a, b, c, \tau_1, \tau_2$ are all positive.

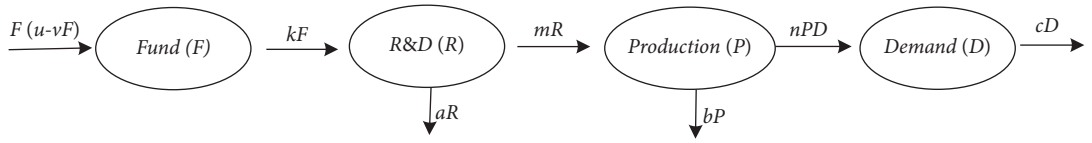

Figure 1: Schematic representation of the process of capital appreciation.

The first equation in model (1) is mathematically equivalent to

$$F(t) = F(0)\exp\left\{\int_0^t [u - k - vF(s)]\mathrm{d}t\right\}. \tag{2}$$

Hence, if $F(0) > 0$, then it follows that $F(t) > 0$. The same conclusion can be drawn that if $D(0) > 0$, then $D(t) > 0$.

Remark 1. $R(t)$ and $P(t)$ can exhibit both negative and positive values. When $R(t)$ and $P(t)$ exhibit negative values, it indicates that the fund is insufficient to satisfy the demands of both R&D as well as production activities. At present, it is imperative to explore alternative funding sources (such as acquiring loans) in order to compensate for the financial deficit.

Note that

$$R_0^4 = \{(F, R, P, D) \mid F \in [0, +\infty), R \in (-\infty, +\infty), P \in (-\infty, +\infty), D \in [0, +\infty)\}. \tag{3}$$

This paper exclusively examines model (1) only on R_0^4. In addition, it is assumed that model (1) satisfies the following initial conditions:

$$F(t) = \phi_1(\theta), R(t) = \phi_2(\theta), P(t) = \phi_3(\theta), D(t) = \phi_4(\theta), \tag{4}$$

where $(\phi_1(\theta), \phi_2(\theta), \phi_3(\theta), \phi_4(\theta)) \in C([-\tau, 0], R_0^4), \phi_i(0) > 0, \tau = \max\{\tau_1, \tau_2\}, i = 1, 2, 3, 4.$ $C([-\tau, 0], R_0^4)$ is the Banach space of continuous functions mapping the interval $[-\tau, 0]$ into R_0^4.

According to the existence and uniqueness theorem [19–22] of differential equation solutions, model (1) has a unique solution $(F(t), R(t), P(t), D(t))$ that satisfies the initial conditions (4).

The following conclusions can be obtained by solving the equations
$$\begin{cases} F(u - vF) - kF = 0, \\ kF - aR - mR = 0, \\ mR - bP - nPD = 0, \\ nPD - cD = 0. \end{cases}$$

Model (1) has one zero-equilibrium point $E^0(0, 0, 0, 0)$. If the following assumptions

$$H_1\colon u - k > 0, H_2\colon \mathrm{kmn}(u - k) - \mathrm{bcv}(a + m) > 0, \tag{5}$$

hold on, there exists a unique positive equilibrium point $E^*(F^*, R^*, P^*, D^*)$, where

$$\begin{aligned} F^* &= \frac{u - k}{v}, \\ R^* &= \frac{k(u - k)}{v(a + m)}, \\ P^* &= \frac{c}{n}, \\ D^* &= \frac{\mathrm{kmn}(u - k) - \mathrm{bcv}(a + m)}{\mathrm{cnv}(a + m)}. \end{aligned} \tag{6}$$

In contrast to its representation in other disciplines [23, 24], the equilibrium point E^* in this paper represents the steady-state values of capital, research and development, production, and demand within an investment project. E_0 denotes the absence of any project investment.

Theorem 2. *When $\tau_1 = \tau_2 = 0$, all solutions of model (1) with initial conditions $F(0) > 0, R(0) > 0, P(0) > 0, D(0) > 0$ are positive for all $t \geq 0$.*

Proof. When $\tau_1 = \tau_2 = 0$, model (1) can be transformed into the following equations:

$$\begin{cases} \dfrac{\mathrm{d}F}{\mathrm{d}t} = F(t)(u - vF(t)) - kF(t), \\ \dfrac{\mathrm{d}R}{\mathrm{d}t} = kF(t) - aR(t) - mR(t), \\ \dfrac{\mathrm{d}P}{\mathrm{d}t} = mR(t) - bP(t) - nP(t)D(t), \\ \dfrac{\mathrm{d}D}{\mathrm{d}t} = nP(t)D(t) - cD(t). \end{cases} \tag{7}$$

The first equation of model (7) is equivalent to

$$F(t) = F(0)\exp\left\{\int_0^t [u - k - vF(s)]\mathrm{d}s\right\}. \tag{8}$$

Therefore, if $F(0) > 0$, then it follows that $F(t) > 0$. Similarly, it can be proved that if $D(0) > 0$, $D(t) > 0$.

From the second equation of model (7), we can get

$$\left.\frac{\mathrm{d}R}{\mathrm{d}t}\right|_{R=0} = \mathrm{kF} > 0. \tag{9}$$

Therefore, if $R(0) > 0$ then it follows that $R(t) > 0$. Similarly, it can be proved that if $P(0) > 0$, $P(t) > 0$. This ends the proof. □

Theorem 3. *When $\tau_1 = \tau_2 = 0$, all feasible solutions of model (7) with the initial conditions $F(0) > 0, R(0) > 0, P(0) > 0, D(0) > 0$ are bounded and enter the region*

$$\Omega_\varepsilon = \left\{(F, R, P, D) \in R_+^4 \colon F + R + P + D \le \frac{u}{v} + \varepsilon, \forall \varepsilon > 0\right\}. \tag{10}$$

Proof. Define a function

$$V(t) = F(t) + R(t) + P(t) + D(t), \tag{11}$$

such that

$$\begin{aligned}\frac{\mathrm{d}V}{\mathrm{d}t} &= F(t)(u - vF(t)) - kF(t) - aR(t) - bP(t) \\ &\quad - cD(t) < F(t)(u - vF(t)).\end{aligned} \tag{12}$$

According to the comparison principle [21], we can obtain

$$\limsup_{t \longrightarrow +\infty} V(t) \le \frac{u}{v}. \tag{13}$$

Thus, $V(t) \le (u/v) + \varepsilon$, as $t \longrightarrow +\infty$. It implies that the region

$$\Omega_\varepsilon = \left\{(F, R, P, D) \in R_+^4 \colon F + R + P + D \le \frac{u}{v} + \varepsilon, \forall \varepsilon > 0\right\}, \tag{14}$$

is a positively invariant set of the model (7). The proof is completed.

The characteristic equation of model (1) at the positive equilibrium point E^* is

$$\left|J(F^*, R^*, P^*, D^*) - \lambda E\right| = \begin{vmatrix} -vF^* - \lambda & 0 & 0 & 0 \\ k & -a - \mathrm{m}e^{-\lambda\tau_1} - \lambda & 0 & 0 \\ 0 & \mathrm{m}e^{-\lambda\tau_1} & -b - nD^*e^{-\lambda\tau_2} - \lambda & -c \\ 0 & 0 & nD^*e^{-\lambda\tau_2} & -\lambda \end{vmatrix} = 0. \tag{15}$$

That is

$$(\lambda + vF^*)\left(\lambda + a + \mathrm{m}e^{-\lambda\tau_1}\right)\left[\lambda^2 + \left(b + nD^*e^{-\lambda\tau_2}\right)\lambda + ncD^*e^{-\lambda\tau_2}\right] = 0. \tag{16}$$

□

Theorem 4

(1) *When* $\tau_1 = \tau_2 = 0$, if assumptions H_1, H_2 hold on, the positive equilibrium E^* *is locally asymptotically stable.*

(2) *When* $\tau_1 = \tau_2 = 0$ and $u - k < 0$, *the zero-equilibrium point* E^0 *is locally asymptotically stable.*

Proof

(1) When $\tau_1 = \tau_2 = 0$, equation (16) is transformed into

$$(\lambda + vF^*)(\lambda + a + m)\left[\lambda^2 + (b + nD^*)\lambda + ncD^*\right] = 0. \tag{17}$$

Let $\lambda_i (i = 1, 2, 3, 4)$ be roots of equation (17), it has

$$\begin{aligned}&\lambda_1 = -vF^* < 0, \lambda_2 = -(\alpha + m) < 0, \\ &\lambda_3 + \lambda_4 = -(b + nD^*) < 0, \lambda_3\lambda_4 = ncD^* > 0.\end{aligned} \tag{18}$$

Therefore, all roots of equation (17) have negative real parts. According to the Hurwitz theorem [12–14], it is well-established that the positive equilibrium point E^* exhibits local asymptotic stability when $\tau_1 = \tau_2 = 0$.

(2) When $\tau_1 = \tau_2 = 0$, the characteristic equation of model (1) at the zero-equilibrium point E^0 is

$$(u - k - \lambda)(a + m + \lambda)(b + \lambda)(c + \lambda) = 0. \tag{19}$$

The solutions to the above equation are as follows:

$$\lambda_1 = u - k, \lambda_2 = -(a + m), \lambda_3 = -b, \lambda_4 = -c. \tag{20}$$

Therefore, when $u - k < 0$, the zero-equilibrium point is locally asymptotically stable.

The proof is finished. □

3. Existence and Local Stability of Hopf Bifurcations

Theorem 5. *If the assumptions $\tau_1 > 0, \tau_2 = 0, H_1, H_2$ and H_3: $m - a > 0$ hold, there exists $\tau_{10} > 0$, which makes the following conclusions true. The model (1) is locally asymptotically stable at the positive equilibrium point E^* when $\tau_1 \in [0, \tau_{10})$ and unstable when $\tau_1 > \tau_{10}$. Model (1) undergoes a Hopf bifurcation at E^* when $\tau_1 = \tau_{10}$.*

Proof. When $\tau_1 > 0, \tau_2 = 0$, the transformation of equation (16) can be expressed as the following equation:

$$\left(\lambda + vF^*\right)\left(\lambda + a + me^{-\lambda\tau_1}\right)\left[\lambda^2 + \left(b + nD^*\right)\lambda + ncD^*\right] = 0. \tag{21}$$

According to the proof process of Theorem 4, equation (21) has three roots with negative real part, and the other root that satisfies the following equation:

$$\lambda + a + me^{-\lambda\tau_1} = 0. \tag{22}$$

Let $\lambda = \omega_1 i\,(\omega_1 > 0)$ be the solution of equation (22), then the following form can be obtained:

$$\omega_1 i + a + m\left[\cos\left(\omega_1\tau_1\right) - i\sin\left(\omega_1\tau_1\right)\right] = 0. \tag{23}$$

Separating the real and imaginary parts from the above equation, we get

$$\begin{aligned} \cos\left(\omega_1\tau_1\right) &= -\frac{a}{m}, \\ \sin\left(\omega_1\tau_1\right) &= \frac{\omega_1}{m}. \end{aligned} \tag{24}$$

It follows that ω_1 satisfies

$$\omega_1^2 = m^2 - a^2. \tag{25}$$

If assumption H_3 holds, the equation (26) has at least one positive root ω_{10}. By substituting ω_{10} into (25), we can get

$$\tau_{1l} = \frac{2n\pi}{\omega_{10}} + \frac{1}{\omega_{10}}\arccos\left(-\frac{a}{m}\right), \quad l = 0, 1, 2, \cdots. \tag{26}$$

Assume that τ_{10} is the smallest positive value in τ_{1l}. Taking the derivative of τ_1 at both ends of equation (22), we can get

$$\left(\frac{d\lambda}{d\tau_1}\right)^{-1} = \frac{e^{\lambda\tau_1}}{\lambda m} - \frac{\tau_1}{\lambda}. \tag{27}$$

Substituting $\lambda = \omega_{10}$ into the above formula, we can obtain

$$\operatorname{Re}\left\{\left(\frac{d\lambda}{d\tau_1}\right)^{-1}\Bigg|_{\tau_1=\tau_{10},\lambda=\omega_{10}i}\right\} = \frac{\sin\left(\omega_{10}\tau_{10}\right)}{m\omega_{10}} = \frac{1}{m^2} > 0. \tag{28}$$

According to the Hopf bifurcation theorem [12, 16–25], Theorem 5 holds. The proof is completed. □

Theorem 6. *If the assumptions $\tau_1 = 0, \tau_2 > 0$, H_1, H_2, and H_4: $2\mathrm{bcv}(a + m) - \mathrm{kmn}(u - k) < 0$ hold, there exists $\tau_{20} > 0$, which makes the following conclusion true. When $\tau_2 \in [0, \tau_{20})$, the positive equilibrium point E^* is locally stable. When $\tau_2 > \tau_{20}$, E^* lose stable, model (1) undergoes a Hopf bifurcation when $\tau_2 = \tau_{20}$.*

Proof. If $\tau_1 = 0, \tau_2 > 0$, equation (17) can be transformed into

$$\left(\lambda + vF^*\right)(\lambda + a + m)\left[\lambda^2 + \left(b + nD^*e^{-\lambda\tau_2}\right)\lambda + ncD^*e^{-\lambda\tau_2}\right] = 0. \tag{29}$$

It is easy to know that equation (29) has two negative real roots, and the remaining two roots satisfy the following equation:

$$\lambda^2 + b\lambda + nD^*(\lambda + c)e^{-\lambda\tau_2} = 0. \tag{30}$$

Let $\lambda = \omega_2 i\,(\omega_2 > 0)$ be the root of equation (30), it has

$$-\omega_2^2 + b\omega_2 i + nD^*\left(\omega_2 i + c\right)\left[\cos\left(\omega_2\tau_2\right) - i\sin\left(\omega_2\tau_2\right)\right] = 0. \tag{31}$$

Separating the real and imaginary parts of the above equation, then there is

$$\begin{cases} -\omega_2^2 + cnD^*\cos\left(\omega_2\tau_2\right) + \omega_2 nD^*\sin\left(\omega_2\tau_2\right) = 0, \\ b\omega_2 + \omega_2 nD^*\cos\left(\omega_2\tau_2\right) - cnD^*\sin\left(\omega_2\tau_2\right) = 0. \end{cases} \tag{32}$$

By eliminating $\cos(w\tau)$ and $\sin(w\tau)$ from formula (32), we can get

$$\omega_2^4 + \left[b^2 - \left(nD^*\right)^2\right]\omega_2^2 - \left(cnD^*\right)^2 = 0. \tag{33}$$

Because assumption H_4 holds

$$b^2 - \left(nD^*\right)^2 = \frac{2\mathrm{bcv}(a + m) - \mathrm{kmn}(u - k)}{\mathrm{cv}(a + m)} \cdot \left(b + nD^*\right) < 0. \tag{34}$$

Furthermore, equation (33) has at least one positive root ω_{20}, substituting ω_{20} into equation (32), we get

$$\tau_{2l} = \frac{2n\pi}{\omega_{20}} + \frac{1}{\omega_{20}}\arccos\left(\frac{(c - b)\omega_{20}^2}{nD^*\left(c^2 + \omega_{20}^2\right)}\right), \quad l = 0, 1, 2, \cdots. \tag{35}$$

Assume that τ_{20} is the minimum positive value in $\tau_{2l}(l = 0, 1, 2, \cdots)$. Taking the derivative of λ with respect to τ_2 in equation (30), there is

$$\operatorname{Re}\left\{\left(\frac{d\lambda}{d\tau_2}\right)^{-1}\Big|_{\lambda=\omega_{20}i,\tau_2=\tau_{20}}\right\} = \operatorname{Re}\left\{\left[\frac{2}{nD^*(\lambda+c)e^{-\lambda\tau_2}} + \frac{b}{nD^*\lambda(\lambda+c)e^{-\lambda\tau_2}} + \frac{1}{\lambda(\lambda+c)} - \frac{\tau_2}{\lambda}\right]_{\lambda=\omega_{20}i,\tau_2=\tau_{20}}\right\}$$
$$= \frac{2}{nD^*}\cdot\frac{c\cdot\cos(\tau_{20}\omega_{20}) + \omega_{20}\cdot\sin(\tau_{20}\omega_{20})}{c^2+\omega_{20}^2} + \frac{b}{nD^*}\cdot\frac{-\omega_{20}\cdot\cos(\tau_{20}\omega_{20}) + c\cdot\sin(\tau_{20}\omega_{20})}{\omega_{20}\left(\omega_{20}^2+c^2\right)} - \frac{1}{\omega_{20}^2+c^2}. \tag{36}$$

Because $\lambda = \omega_{20}i, \tau_2 = \tau_{20}$ are the solutions of the following equation system (32):

$$c\cdot\cos(\omega_{20}\tau_{20}) + \omega_2\cdot\sin(\omega_{20}\tau_{20}) = \frac{\omega_{20}^2}{nD^*}, -\omega_2\cdot\cos(\omega_2\tau_2) + c\cdot\sin(\omega_2\tau_2) = \frac{b\omega_{20}}{nD^*}. \tag{37}$$

Substituting the above formula into (36), we can obtain

$$Re\left\{\left(\frac{d\lambda}{d\tau_2}\right)^{-1}\Big|_{\lambda=\omega_{20}i,\tau_2=\tau_{20}}\right\} = \frac{2\omega_{20}^2 + b^2 - (nD^*)^2}{(nD^*)^2\left(c^2+\omega_{20}^2\right)} = \frac{\omega_{20}^4 + (cnD^*)^2}{\omega_{20}^2(nD^*)^2\left(c^2+\omega_{20}^2\right)} > 0. \tag{38}$$

Therefore, the conclusion of Theorem 5 holds. This ends the proof.

According to the proof process of Theorems 5 and 6, in conjunction with the characteristic equation (16), we establish the following conclusions. □

Theorem 7. *If assumptions $H_1 - H_4$ hold on, when $\tau_1 \in (0, \tau_{10})$ and $\tau_2 \in (0, \tau_{20})$, the positive equilibrium E^* is locally asymptotically stable; when $\tau_1 \in (0, \tau_{10}), \tau_2 = \tau_{20}$ or $\tau_1 = \tau_{10}, \tau_2 \in (0, \tau_{20})$ or $\tau_1 = \tau_{10}, \tau_2 = \tau_{20}$, model (1) undergoes a Hopf bifurcation. In other cases, E^* loses stability.*

4. Numerical Simulation

In order to validate the accuracy of the analytical conclusions presented in Sections 2 and 3, this section primarily conducts numerical simulations based on model (1). If the parameters

$$u = 5, v = 1.5, k = 3, m = 1, n = 1.5, a = 0.9, b = 1, c = 0.6,$$
$$F(0) = 4, R(0) = 3, P(0) = 2, D(0) = 1. \tag{39}$$

In parameter group (39), with $u = 2$ and all other parameters held constant, the numerical simulation of model (1) is presented in Figure 2. The local asymptotic stability of the zero-equilibrium point is demonstrated in Figure 2 when $\tau_1 = \tau_2 = 0$ and $u - k < 0$.

According to the data in parameter group (39), the verification of the establishment of $H_1 - H_4$ can be readily accomplished. The positive equilibrium point E^* is

$$E^* = (F^*, R^*, P^*, D^*) = (1.33,\ 11,\ 0.40,\ 2.84). \tag{40}$$

Using the formulae (25), (26), (33), and (35), we get

$$\omega_{10} = 0.44, \tau_{10} = 6.17, \omega_{20} = 178, \tau_{20} = 0.41. \tag{41}$$

When $\tau_1 = 0, \tau_2 = 0$, the numerical simulation of model (1) is shown in Figure 3. Figure 3 demonstrates that for $\tau_1 = 0, \tau_2 = 0$, the solution of model (1) exhibit not only boundedness but also local asymptotic stability. The conclusions of Theorems 2 and 3 are confirmed by the findings presented in Figure 3.

When $\tau_1 = 21 < \tau_{10}, \tau_2 = 0$, the numerical simulation of model (1) is shown in Figure 4.

In Figure 4, despite the initial high degree of fluctuation in the moving point, its fluctuations gradually diminish and stabilize over time, thus confirming the validity of Theorem 4's conclusion.

Figures 3 and 4 confirm that the positive equilibrium point of model (1) is locally asymptotically stable when $\tau_1 < \tau_{10}, \tau_2 = 0$.

If $\tau_1 = 6.17 = \tau_{10}, \tau_2 = 0$, the model (1) exhibits periodic solutions that exhibit fluctuations around a positive equilibrium point. E^*, and its numerical simulation is shown in Figure 5.

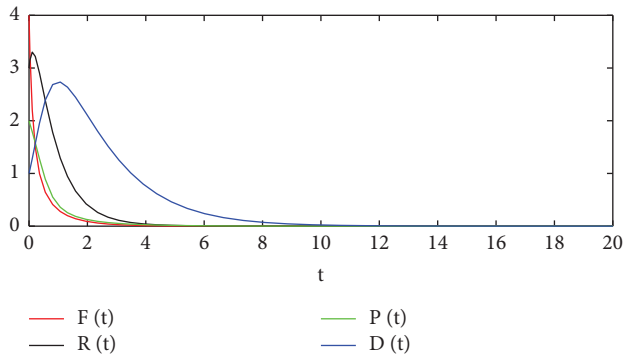

Figure 2: When $\tau_1 = 0, \tau_2 = 0$ and $u - k < 0$, E^0 is locally asymptotically stable.

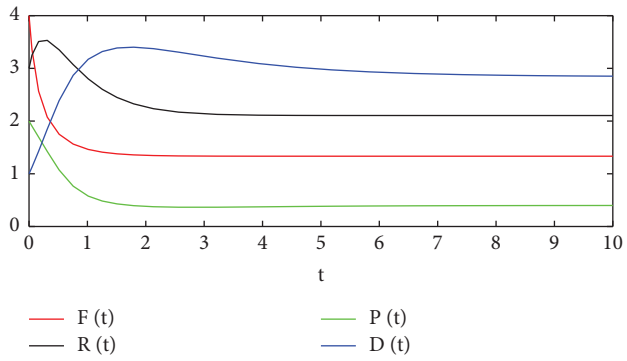

Figure 3: When $\tau_1 = 0, \tau_2 = 0$, E^* is locally asymptotically stable.

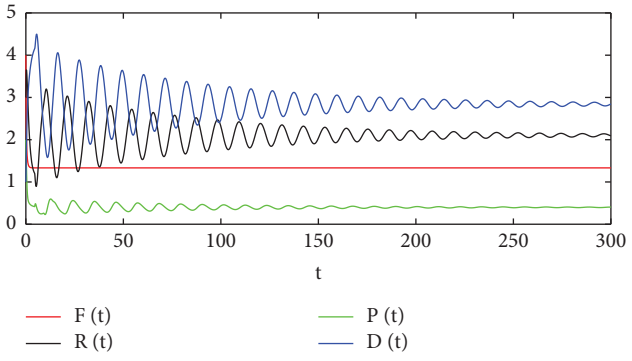

Figure 4: When $\tau_1 = 21, \tau_2 = 0$, E^* is asymptotically stable.

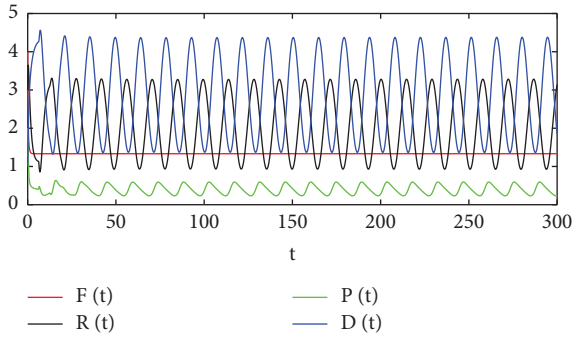

Figure 5: When $\tau_1 = 6.17, \tau_2 = 0$, model (1) has a periodic solution.

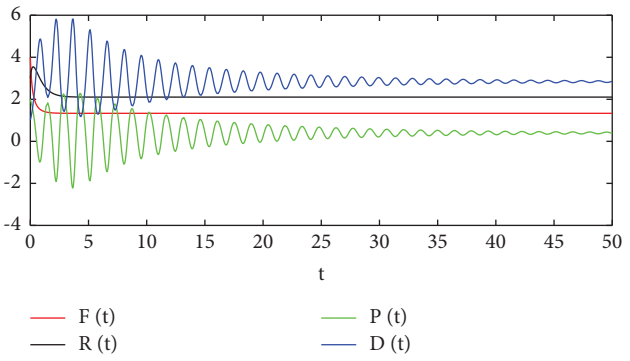

Figure 6: When $\tau_1 = 0, \tau_2 = 0.38$, E^* is locally asymptotically stable.

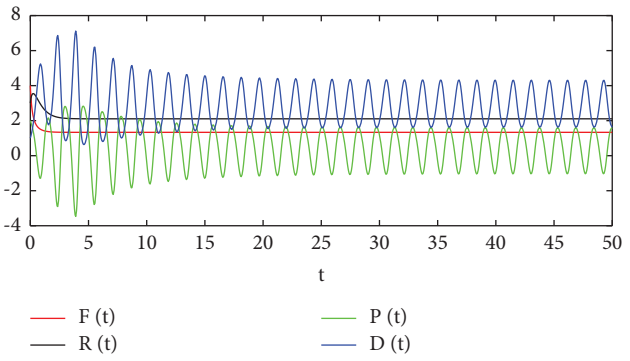

Figure 7: When $\tau_1 = 0, \tau_2 = 0.41$, model (1) has a periodic solution.

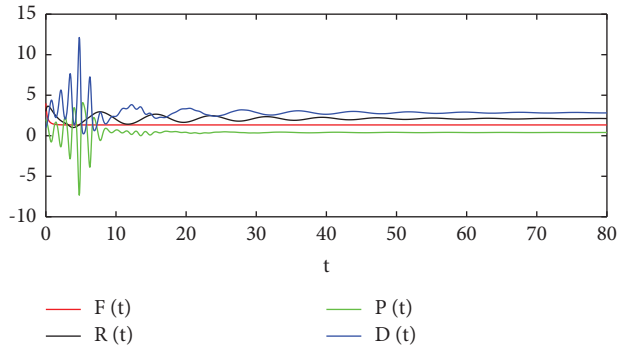

Figure 8: When $\tau_1 = 3, \tau_2 = 0.36$, model (1) has periodic solutions.

Figure 5 shows that the model (1) has a cyclic periodic solution. Specifically, it induces the emergence of a Hopf bifurcation at the positive equilibrium point. The conclusions of Theorem 5 are indirectly validated.

If $\tau_1 = 0, \tau_2 = 0.38 < \tau_{20}$, E^* is locally asymptotically stable, and its numerical simulation is shown in Figure 6. If $\tau_1 = 0, \tau_2 = 0.41 = \tau_{20}$, model (1) has periodic solutions, and its numerical simulation is shown in Figure 7.

The validity of Theorem 6 is confirmed by Figure 6. Specifically, for $\tau_1 = 0$ and $\tau_2 < \tau_{20}$, the positive equilibrium point of model (1) exhibits local asymptotic stability. In the case of $\tau_1 = 0$ and $\tau_2 = \tau_{20}$, model (1) still undergoes Hopf bifurcation near the positive equilibrium point.

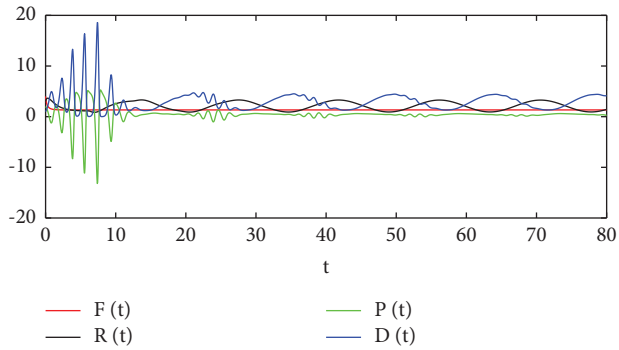

Figure 9: When $\tau_1 = 6.17, \tau_2 = 0.41$, model (1) has periodic solutions.

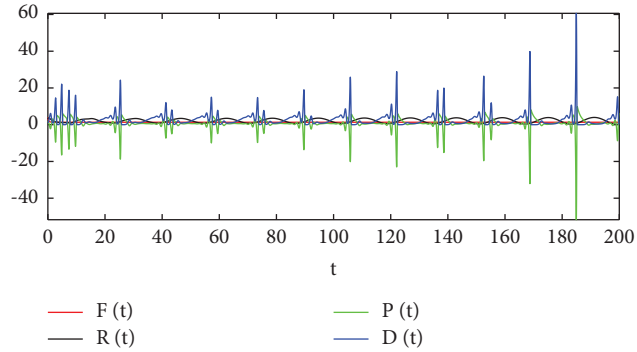

Figure 10: When $\tau_1 = 7, \tau_2 = 0.5$, model (1) loses stability.

If $\tau_1 = 3 < \tau_{10}$ and $\tau_2 = 0.36 < \tau_{20}$, the equilibrium point E^* is locally asymptotically stable, as demonstrated by numerical simulation in Figure 8. However, if $\tau_1 = 6.17 = \tau_{10}$ and $\tau_2 = 0.41 = \tau_{20}$, model (1) undergoes a Hopf bifurcation, as shown in Figure 9. Finally, when $\tau_1 = 7 > \tau_{10}$ and $\tau_2 = 0.5 > \tau_{20}$, E^* loses stability and its numerical simulation is presented in Figure 10.

Figure 8 illustrates that the positive equilibrium point of model (1) is locally asymptotically stable as long as $\tau_1 < \tau_{10}$ and $\tau_2 < \tau_{20}$. However, Figure 9 demonstrates that if $\tau_1 = \tau_{10}$ or $\tau_2 = \tau_{20}$, Hopf bifurcation will occur near the positive equilibrium point in model (1). Moreover, Figure 10 indicates that when either $\tau_1 > \tau_{10}$ or $\tau_2 > \tau_{20}$, the positive equilibrium point of model (1) becomes unstable. The validity of Theorem 7 is confirmed.

As depicted in Figure 3, the investment process exhibits minimal dynamic fluctuations when both the R&D cycle (τ_1) and the production cycle (τ_2) are set to zero. It is evident from Figures 3, 5, and 7 that the investment dynamics tend to exhibit stability over time when both the R&D cycle τ_1 and the production cycle τ_2 are less than their respective thresholds of τ_{10} and τ_{20}. Figures 4, 6, and 8 demonstrate that when the R&D cycle ($\tau_1 = \tau_{10}$) or the production cycle ($\tau_2 = \tau_{20}$), remain constant, cyclic fluctuations occur in the R&D quantity, production quantity, and demand quantity despite a consistent investment fund allocation. Figure 10 illustrates that as the R&D cycle τ_1 exceeds τ_{10} and the production cycle τ_2 surpasses τ_{20}, there will be an increasingly volatile fluctuation in both production quantity and demand quantity. Furthermore, it is evident that the disparity in production funding will continue to widen, ultimately resulting in investment failure. Likewise, in cases where the R&D cycle τ_1 exceeds τ_{10} or the production cycle τ_2 surpasses τ_{20}, the investment will also prove unsuccessful.

The aforementioned analysis demonstrates that the R&D and production cycles exert a decisive influence on the dynamic trajectory of investment projects.

Subsequently, we will investigate the impact of parameter modifications on the model through numerical simulations. The alteration of parameters has two primary impacts on the model, specifically, the impact on the equilibrium point and the impact on the degree of oscillation in the integral curve.

Furthermore, the fluctuation degree of the integral curve is also influenced by time delays τ_1 and τ_2. It is easy to know that the oscillation amplitude and width of the integral curve are positively correlated with τ_1 and τ_2, as depicted in Figures 3–9.

Under the conditions of $H_1 - H_2$, with $\tau_1 = \tau_2 = 0$ and an unchanged initial value, we examine the impact on model (1), resulting from changes in parameter set (42).

In parameter group (42), the value of parameter u ranges from 4 to 7 in increments of 0.5, and Figure 11 displays the numerical simulation results of model (1) under this condition while keeping other parameters constant. The alterations in the positive equilibrium point are presented in Table 1.

As depicted in Figure 11, the length and width of the amplitude remained relatively stable as u increased. However, significant changes have occurred in the equilibrium

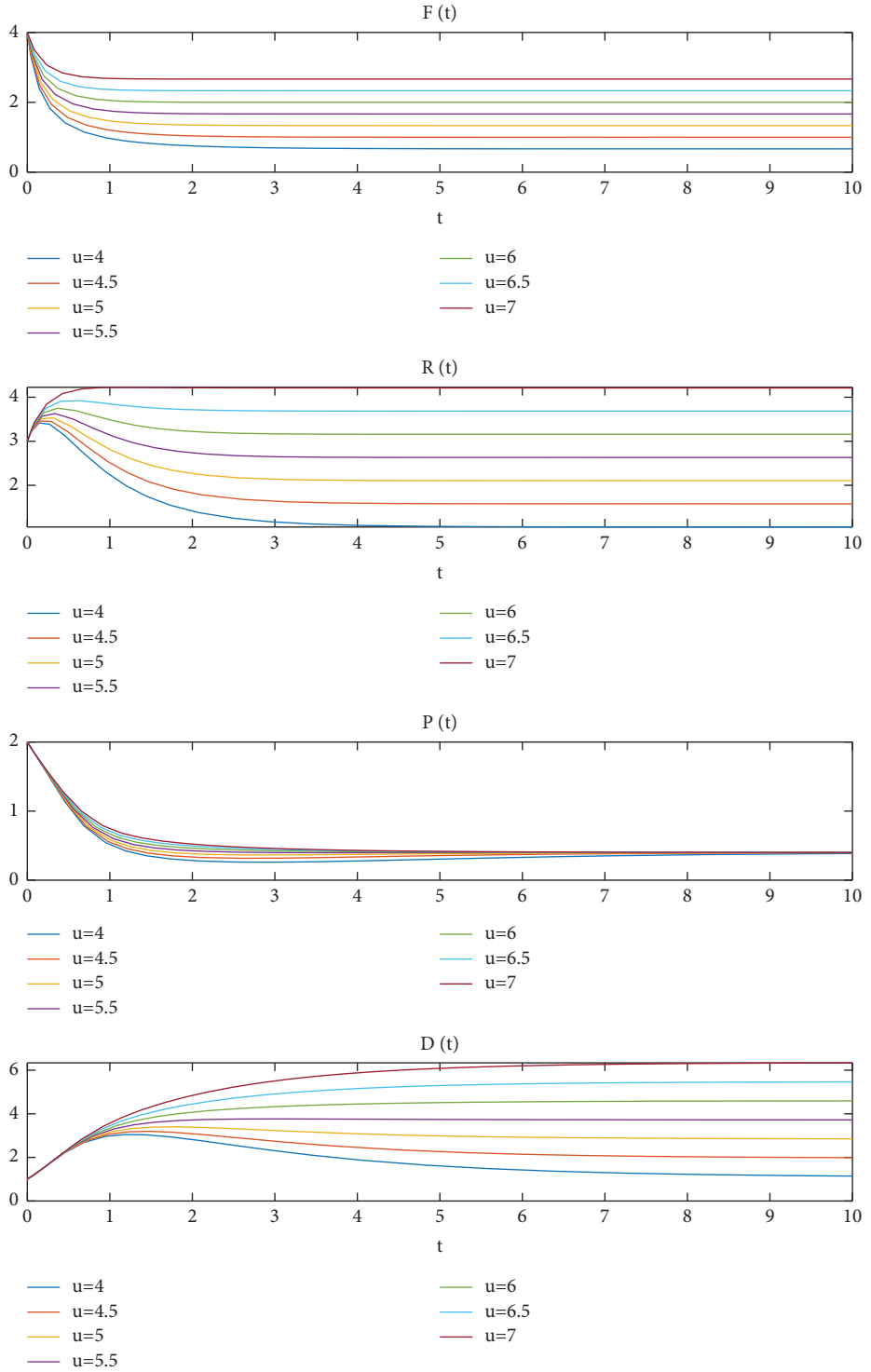

Figure 11: Numerical simulation diagram of model (1), when $\tau_1 = \tau_2 = 0, u = 4: 0.5: 7$.

Table 1: As the value of u increases, $E^*(F^*, R^*, P^*, D^*)$ are the corresponding values.

u	4	4.5	5	5.5	6	6.5	7
F^*	0.67	1	1.33	1.67	2	2.33	2.67
R^*	1.05	1.58	2.11	2.63	3.16	3.68	4.21
P^*	0.40	0.40	0.40	0.40	0.40	0.40	0.40
D^*	1.09	1.96	2.84	3.72	4.60	5.47	6.35

Table 2: The associations between equilibrium points (F^*, R^*, P^*, D^*) and incremental parameters.

	u	v	k	m	n	a	b	c
F^*	Increase	Decrease	Decrease	Constant	Constant	Constant	Constant	Constant
R^*	Increase	Decrease	Nonmonotonicity	Decrease	Constant	Decrease	Constant	Constant
P^*	Constant	Constant	Constant	Constant	Decrease	Constant	Constant	Increase
D^*	Increase	Decrease	Nonmonotonicity	Increase	Increase	Decrease	Decrease	Decrease

point, as evidenced by the specific value alterations presented in Table 1. It is easy to know that F^*, R^*, D^* increase with the increase of u, while the value of P^* remains the same.

Similarly, it can be observed that when the remaining parameters are held constant and only one parameter is incrementally adjusted, the shape of $F(t), R(t), P(t)$, and $D(t)$ curves will remain relatively stable. However, the equilibrium point $E^*(F^*, R^*, P^*, D^*)$ undergoes changes under various circumstances, as detailed in Table 2.

The aforementioned analysis assumes that variations in the parameters u, v, k, m, n, a, b, and c exert minimal influence on the fluctuations of the curves $F(t), R(t), P(t)$, and $D(t)$. However, their impact on the equilibrium point is substantial. The magnitude of the delay in model (1) is a determining factor for the level of volatility, ascertaining its significance.

5. Properties of the Hopf Bifurcation

Based on the aforementioned analysis, it can be inferred that model (1) experiences a Hopf bifurcation at E^* when either $\tau_1 = \tau_{10}$ or $\tau_2 = \tau_{20}$. The normal form theory and the center manifold theory [25, 26] are employed in this section to investigate the properties of Hopf bifurcation for model (1) at the positive equilibrium point E^*. Without loss of generality, this paper exclusively focuses on the branch direction of Hopf bifurcation and the stability of the corresponding periodic solution in model (1) when $\tau_1 = \tau_{10}, \tau_2 \in [0, \tau_{10}]$.

Let $t \longrightarrow t/\tau_1, u_1(t) = F(\tau_1 t) - F^*, u_2(t) = R(\tau_1 t) - R^*, u_3(t) = P(\tau_1 t) - P^*, u_4(t) = D(\tau_1 t) - D^*, \tau_1 = \tau_{10} + \mu, \mu \in \mathscr{R}$, then model (1) can be transformed into

$$\begin{cases} \dfrac{\mathrm{d}u_1(t)}{\mathrm{d}t} = (\tau_{10}+\mu)\left[-vF^*u_1(t) - vu_1^2(t)\right], \\ \dfrac{\mathrm{d}u_2(t)}{\mathrm{d}t} = (\tau_{10}+\mu)\left[ku_1(t) - au_2(t) - mu_2(t-1)\right], \\ \dfrac{\mathrm{d}u_3(t)}{\mathrm{d}t} = (\tau_{10}+\mu)\left[-bu_3(t) - nP^*u_4(t) - nD^*u_3\left(t-\dfrac{\tau_2}{\tau_1}\right) + mu_2(t-1) - nu_3\left(t-\dfrac{\tau_2}{\tau_1}\right)u_4(t)\right], \\ \dfrac{\mathrm{d}u_4(t)}{\mathrm{d}t} = (\tau_{10}+\mu)\left[nD^*u_3\left(t-\dfrac{\tau_2}{\tau_1}\right) + nu_3\left(t-\dfrac{\tau_2}{\tau_1}\right)u_4(t)\right]. \end{cases} \tag{42}$$

Since the calculation process described in this paper closely follows that of article [18], only the essential calculation formulae are presented herein.

The following are the build functions:

$$L(\mu, \phi) = (\tau_{10}+\mu)\left(A_0\phi(0) + B_0\phi\left(-\frac{\tau_2}{\tau_1}\right) + C_0\phi(-1)\right),$$

$$F(\mu, \phi) = (\tau_{10}+\mu)\begin{pmatrix} -v\phi_1^2(0) \\ 0 \\ 0 \\ 0 \end{pmatrix},$$

$$A_0 = \begin{pmatrix} -vF^* & 0 & 0 & 0 \\ k & -a & 0 & 0 \\ 0 & 0 & -b & -nP^* \\ 0 & 0 & 0 & 0 \end{pmatrix},$$
$$B_0 = \begin{pmatrix} 0 & 0 & 0 & 0 \\ 0 & 0 & 0 & 0 \\ 0 & 0 & -nD^* & 0 \\ 0 & 0 & nD^* & 0 \end{pmatrix}, \tag{43}$$
$$C_0 = \begin{pmatrix} 0 & 0 & 0 & 0 \\ 0 & -m & 0 & 0 \\ 0 & m & 0 & 0 \\ 0 & 0 & 0 & 0 \end{pmatrix},$$

where $\phi = (\phi_1(\theta), \phi_2(\theta), \phi_3(\theta), \phi_4(\theta)) \in C([-1, 0], \mathscr{R}^4)$. Then, equation (42) can be reformulated as the vector differential equation [18, 27–29] $\dot{u}(t) = L_\mu(u_t) + F(\mu, u_t)$.

Let $q(\theta) = (1, q_1, q_2, q_3)^T \exp(i\omega_{10}\tau_{10}\theta)$ be the eigenvector of $A(0)$ corresponding to $i\omega_0$ and $q^*(s) = D_0 (1, q_1^*, q_2^*, q_3^*)^T \exp(i\omega_{10}\tau_{10}s)$ be the eigenvector of $A^*(0)$ corresponding to $-i\omega_{10}$, then there are

$$\begin{aligned} &(A_0 + B_0 \exp(-i\omega_{10}\tau_{10}) + C_0 \exp(-i\omega_{10}\tau_{10}) - i\omega_{10}E_0)q(0) = (0, 0, 0, 0)^T, \\ &(q^*(0))^T (A_0 + B_0 \exp(-i\omega_{10}\tau_{10}) + C_0 \exp(-i\omega_{10}\tau_{10}) + i\omega_{10}E_0) = (0, 0, 0, 0), \end{aligned} \tag{44}$$

where E_0 is the identity matrix.

By solving the above two matrix equations, we can obtain

$$\begin{aligned} &q_1 = \frac{k}{a + m\exp(-i\omega_{10}\tau_{10}) + i\omega_{10}}, q_2 = \frac{a_{22}m\exp(-i\omega_{10}\tau_{10})}{a_{11}a_{22} - a_{12}a_{21}}q_1, q_3 = -\frac{a_{21}m\exp(-i\omega_{10}\tau_{10})}{a_{11}a_{22} - a_{12}a_{21}}q_1, \\ &q_1^* = \frac{vF^* - i\omega_{10}}{k}, q_2^* = \frac{a + m\exp(-i\omega_{10}\tau_{10}) - i\omega_{10}}{m\exp(-i\omega_{10}\tau_{10})}q_1^*, q_3^* = \frac{nP^*}{i\omega_{10}}q_2^*, \end{aligned} \tag{45}$$

where

$$a_{11} = b + nD^*\exp(-i\omega_{10}\tau_{10}) + i\omega_{10}, a_{12} = nP^*, a_{21} = nD^*\exp(-i\omega_{10}\tau_{10}), a_{22} = -i\,\omega_{10}. \tag{46}$$

The essential formula [18] for calculation is presented as follows:

$$g_{20} = -2\tau_{10}\overline{D}v, g_{11} = -2\tau_{10}\overline{D}v, g_{02} = -2\tau_{10}\overline{D}v, g_{21} = -2\tau_{10}\overline{D}v\left(W_{20}^{(1)}(0) + 2W_{11}^{(1)}(0)\right). \tag{47}$$

In the expression of g_{21}, it is necessary to calculate $W_{20}(\theta), W_{11}(\theta), \theta \in [-1, 0]$. According to the calculation process in references [18, 27–29],

$$W_{20}(\theta) = \frac{g_{20}q(0)}{-i\omega_{10}\tau_{10}}\exp\left(i\omega_{10}\tau_{10}\theta\right) + \frac{\overline{g}_{20}\overline{q}(0)}{-3i\omega_{10}\tau_{10}}\exp\left(-i\omega_{10}\tau_{10}\theta\right) + E_1\exp\left(2i\omega_{10}\tau_{10}\theta\right),$$
$$W_{11}(\theta) = \frac{g_{11}q(0)}{i\omega_{10}\tau_{10}}\exp\left(i\omega_{10}\tau_{10}\theta\right) + \frac{\overline{g}_{11}\overline{q}(0)}{-i\omega_{10}\tau_{10}}\exp\left(-i\omega_{10}\tau_{10}\theta\right) + F_1, \tag{48}$$

where

$$\left[A_0 + (B_0 + C_0)e^{-2i\omega_{10}\tau_{10}} - 2i\omega_{10}E_0\right]E_1 = -2\begin{pmatrix} -\nu \\ 0 \\ 0 \\ 0 \end{pmatrix}, (A_0 + B_0 + C_0)F_1 = -\begin{pmatrix} -\nu \\ 0 \\ 0 \\ 0 \end{pmatrix}. \tag{49}$$

So, we get

$$E_1 = 2\begin{pmatrix} -\nu F^* - 2i\omega_{10} & 0 & 0 & 0 \\ k & -a - me^{-2i\omega_{10}\tau_{10}} - 2i\omega_{10} & 0 & 0 \\ 0 & me^{-2i\omega_{10}\tau_{10}} & -b - nD^*e^{-2i\omega_{10}\tau_{10}} - 2i\omega_{10} & -nP^* \\ 0 & 0 & nD^*e^{-2i\omega_{10}\tau_{10}} & -2i\omega_{10} \end{pmatrix}^{-1}\begin{pmatrix} \nu \\ 0 \\ 0 \\ 0 \end{pmatrix},$$
$$F_1 = \begin{pmatrix} -\nu F^* & 0 & 0 & 0 \\ k & -a - m & 0 & 0 \\ 0 & m & -nD^* - b & -nP^* \\ 0 & 0 & nD^* & 0 \end{pmatrix}^{-1}\begin{pmatrix} \nu \\ 0 \\ 0 \\ 0 \end{pmatrix}. \tag{50}$$

In summary, the key parameters $g_{20}, g_{11}, g_{02}, g_{21}$ can be represented by the parameters in model (1). Then the following parameters [18, 27–29] can be calculated:

$$c_1(0) = \frac{i}{2m_{10}\tau_{10}}\left(g_{20}g_{11} - 2\left|g_{11}\right|^2 - \frac{1}{3}\left|g_{02}\right|^2\right) + \frac{g_{21}}{2},$$
$$\mu_2 = -\frac{Re\{c_1(0)\}}{Re\left\{\lambda'(\tau_{10})\right\}}, \beta_2 = 2\mathrm{Re}\{c_1(0)\}, T_2 = -\frac{Im\{c_1(0)\} + \mu_2 Im\left\{\lambda'(\tau_{10})\right\}}{m_{10}\tau_{10}}. \tag{51}$$

Theorem 8. *For model (1), if $H_1 - H_4$ hold, then*

(1) if $\mu_2 > 0$ ($\mu_2 < 0$), then the Hopf bifurcation is supercritical (subcritical).

(2) if $\beta_2 < 0$ ($\beta_2 > 0$), then the bifurcating periodic solutions are stable (unstable).

(3) if $T_2 > 0$ ($T_2 < 0$), then the period of the bifurcating periodic solutions increases (decreases).

6. Conclusions

This paper presented a practical differential dynamics model with two hysteresis based on the direction of investment fund flows and value growth processes. The analysis of the model yielded several conclusions.

(1) The realization of investment profits is contingent upon the effective supply of products to meet demand.

(2) The duration of research and development (R&D) as well as production significantly influenced the outcome of investments, potentially leading to either success or failure. To ensure successful investment, it was imperative to rigorously control the maximum time allocated for R&D and production.

(3) When cyclic dynamics occurred in R&D, production, or demand quantities, it may indicate a potential investment failure. Therefore, shortening the R&D and production time was necessary.

However, the research method used in this study has certain limitations, mainly due to its reliance on theoretical construction and model analysis. For example, the coefficients within the model have not yet been determined based on empirical data, and further exploration is needed to control the parameters within a more favorable range. The future research direction involves designing or applying algorithms for parameter estimation, while further investigation is needed to explore how to achieve parameter control in this paper.

Data Availability

The data used to support the findings of this study are included within the article.

Conflicts of Interest

The author declares that there are no conflicts of interest.

Acknowledgments

This work was supported by the Heilongjiang Bayi Agricultural University Talent Support Program Project (RRCLG201902).

References

[1] E. Vigna and S. Haberman, "Optimal investment strategy for defined contribution pension schemes," *Insurance: Mathematics and Economics*, vol. 28, no. 2, pp. 233–262, 2001.

[2] S. Haberman and E. Vigna, "Optimal investment strategies and risk measures in defined contribution pension schemes," *Insurance: Mathematics and Economics*, vol. 31, no. 1, pp. 35–69, 2002.

[3] R. J. Thomson, "The use of utility functions for investment channel choice in defined contribution retirement funds, I: defence," *British Actuarial Journal*, vol. 9, no. 3, pp. 653–709, 2003.

[4] J. Cox, S. A. C. Ross, and S. A. Ross, "The valuation of options for alternative stochastic processes," *Journal of Financial Economics*, vol. 3, no. 1-2, pp. 145–166, 1976.

[5] S. L. Heston, "A closed-form solution for options with stochastic volatility with applications to bond and currency options," *Review of Financial Studies*, vol. 6, no. 2, pp. 327–343, 1993.

[6] X. Lin and Y. F. Yang, "Optimal investment for defined contribution pension plans under Heston model," *Mathematica Applicata*, vol. 2, pp. 413–418, 2010.

[7] C. B. Zhang, X. M. Rong, and R. J. Hou, "ect., "Investment portfolio optimization for fefined-contributon pension under a Heston model," *Systems Engineering*, vol. 30, no. 12, pp. 39–44, 2012.

[8] A. Matsumoto and F. Szidarovszky, "Continuous Hicksian trade cycle model with consumption and investment time delays," *Journal of Economic Behavior & Organization*, vol. 75, no. 1, pp. 95–114, 2010.

[9] T. Asada, C. Douskos, and P. Markellos, "Numerical exploration of kaldorian macrodynamics: hopf-neimark bifurcations and business cycles with fixed exchange rates," *Discrete Dynamics in Nature and Society*, vol. 2007, Article ID 98059, 16 pages, 2007.

[10] X. P. Wu and L. Wang, "Multi-parameter bifurcations of the kaldor–kalecki model of business cycles with delay," *Nonlinear Analysis: Real World Applications*, vol. 11, no. 2, pp. 869–887, 2010.

[11] F. Xu and S. M. Li, "The stability analysis of the enterprise competition model with two time delays," *Journal of Jiangxi Normal University (Natural Science)*, vol. 45, pp. 518–526, 2018.

[12] N. Toshioki, H. Tadayuki, and H. Yoshiyuki, *Differential Equations with Time Lag-Introduction to Functional Differential Equations*, Science Press, Beijing, China, 2019.

[13] R. Xu, X. H. Tian, and Q. T. Gan, *Modeling and Analysis of Infectious Disease Dynamics*, Science Press, Beijing, China, 2019.

[14] Z. J. Xu, Z. H. Zu, and Q. Xu, "Research Progress on dynamic modeling of infectious diseases," *Military Medicine*, vol. 35, no. 11, pp. 1–6, 2011.

[15] Z. P. Wei, *Dynamic Analysis of Infectious Disease Model with Nonlinear Disease Incidence*, Southwest University, Chongqing, China, 2019.

[16] H. S. Dong and S. X. Zhang, "Study on a vector infectious disease model with impulsive disturbance and saturated cure rate," *Journal of Xi'an University of Technology*, vol. 35, no. 1, pp. 98–105, 2019.

[17] J. Q. Li, F. Wang, and Z. E. Ma, "Global analysis of an infectious disease model with isolation," *Journal of Engineering Mathematics*, vol. 21, pp. 20–24, 2005.

[18] D. B. Gao, "Dynamic System analysis of investment in both production and R&D with time delay," *Journal of Mathematics*, vol. 2022, Article ID 1116671, 12 pages, 2022.

[19] Z. E. Ma, Y. C. Zhou, and C. Z. Li, *Qualitative and Stable Methods of Ordinary Differential Equations*, Science Press, Beijing, China, 2015.

[20] J. Y. Zhang, *Geometric Theory and Bifurcation Problems of Ordinary Differential Equations*, Peking University Press, Beijing, China, 1981.

[21] L. S. Chen, *Mathematical Ecology Models and Research Methods*, Science Press, Beijing, China, 2017.

[22] J. J. Wei, H. B. Wang, and W. H. Jiang, *Branch Theory and Application of Delay Differential Equation*, Science Press, Beijing, China, 2012.

[23] M. H. Khoobkar, M. D. T. Fooladi, and M. H. Rezvani, "Partial offloading with stable equilibrium in fog-cloud environments using replicator dynamics of evolutionary game theory," *Cluster Computing*, vol. 25, no. 2, pp. 1393–1420, 2022.

[24] C. Li, "Hopf bifurcation and parameter sensitivity analysis of a doubly-fed variable-speed pumped storage unit," *Energies*, vol. 2021, no. 15, Article ID 15010204, 2021.

[25] B. D. Hassard, N. D. Kazarinoff, and Y. H. Wan, *Theory and Applications of Hopf Bifurcation*, Cambridge University Press, Cambridge, UK, 1981.

[26] J. I. Richards and H. K. Youn, *Theory of Distributions: A Nontechnical Introduction*, Cambridge University Press, Cambridge, UK, 1995.

[27] Y. X. Dai, Y. P. Lin, and H. T. Zhao, "Hopf bifurcation and global periodic solutions in a predator-prey system with michaelis-menten type functional response and two delays," *Abstract and Applied Analysis*, vol. 2014, Article ID 835310, 16 pages, 2014.

[28] X. G. Li, S. G. Ruan, and J. J. Wei, "Stability and bifurcation in delay–differential equations with two delays," *Journal of Mathematical Analysis and Applications*, vol. 236, no. 2, pp. 254–280, 1999.

[29] Y. L. Song, M. A. Han, and Y. H. Peng, "Stability and Hopf bifurcations in a competitive Lotka–Volterra system with two delays," *Chaos, Solitons & Fractals*, vol. 22, no. 5, pp. 1139–1148, 2004.